Calonne, N., C. Geindreau, F. Flin, S. Morin, B. Lesaffre, S. Rolland du Roscoat and P. Charrier (2012), 3D image-based numerical computations of snow permeability: links to specific surface area, density, and microstructural anisotropy, *The Cryosphere*, submitted.

3D image-based numerical computations of snow permeability: links to specific surface area, density, and microstructural anisotropy

N. Calonne, C. Geindreau, F. Flin, S. Morin, B. Lesaffre,
S. Rolland du Roscoat and P. Charrier.

Auxiliary Materials

Table of Contents and General Information

Table of Contents

General Information

In the following, we provide the list of the samples used in this study with related information (**Table 1**) and values of permeability, density and specific surface area (**Table 2**). For each snow type [*Fierz et al., 2009*], a typical microtomographic sample is presented together with its REV estimate in term of permeability:

- **Figures 1.a – 6.a:** 3-D images of the snow sample. The color levels of the images correspond to the fluid velocity (intensity) computed for a pressure drop of 2×10^{-2} Pa along the vertical direction (z) and a dynamic viscosity of air of 1.8×10^{-5} Pa s^{-1}. The ice grains are represented in white.

- **Figures 1.b – 6.b:** Estimations of the REV (the smallest fraction of the sample volume from which a variable representative of the whole can be determined) with respect to the permeability. The REV is estimated by calculating values of permeability from several sub-volumes of increasing sizes. It is reached as soon as values remain constant when sub-volumes of calculations increase. For each figure, the permeability value computed on the largest volume size corresponds to that given in Table 2.

List of the 35 Samples Used in the Study

Sample name	Snow type	Voxel size (μm^3)	Remarks	Main References
Fr	PP	4.91	Sampled at Col de Porte[1], 14 February 2002.	Calonne et al., 2011
I01	PP	4.91	Sampled at Col de Porte, 15 h after the snowfall.	Flin et al., 2004
I03	PP	4.91	62 h after the snowfall, under isothermal conditions at –2°C.	Flin et al., 2004
I04	PP	4.91	81 h after the snowfall, under isothermal conditions at –2°C.	Flin et al., 2004
I08	DF	4.91	297 h after the snowfall, under isothermal conditions at –2°C.	Flin et al., 2004
I15	RG	4.91	806 h after the snowfall, under isothermal conditions at –2°C.	Flin et al., 2004
I19	RG	4.91	1381 h after the snowfall, under isothermal conditions at –2°C.	Flin et al., 2004
I21	RG	4.91	1694 h after the snowfall, under isothermal conditions at –2°C.	Flin et al., 2004
I23	RG	4.91	2026 h after the snowfall, under isothermal conditions at –2°C.	Flin et al., 2004
P03	PP	8.48	Girose glacier[2], 20 cm depth, 17 March 2009.	Flin et al., 2011
P04	DF	8.588	Girose glacier, 40 cm depth, 17 March 2009.	Flin et al., 2011
P06	RG	6.158	Girose glacier, 60 cm depth, 17 March 2009.	Flin et al., 2011
P07	RG	8.609	Girose glacier, 70 cm depth, 17 March 2009.	Flin et al., 2011
P08	RG	8.552	Girose glacier, 100 cm depth, 17 March 2009.	Flin et al., 2011
P09	RG	6.158	Girose glacier, 120 cm depth, 17 March 2009.	Flin et al., 2011
P10	RG	6.103	Girose glacier, 165 cm depth, 17 March 2009.	Flin et al., 2011
P11	RG	8.588	Girose glacier, 65 cm depth, 1 March 2009.	Flin et al., 2011
P14	RG	6.154	Girose glacier, 80 cm depth, 1 March 2009.	Flin et al., 2011
P15	RG	6.158	Girose glacier, 170 cm depth, 1 March 2009.	Flin et al., 2011
H00	RG	8.609	Sieved snow, followed by isothermal conditions.	Flin et al., 2011
H01	MF	8.609	Grain coarsening of water-saturated snow and drainage after 1h.	Flin et al., 2011
H1-2	MF	8.590	Grain coarsening of water-saturated snow and drainage after 6h.	Flin et al., 2011
H02	MF	8.590	Grain coarsening of water-saturated snow and drainage after 24h.	Flin et al., 2011
H03	MF	8.609	Grain coarsening of water-saturated snow and drainage after 48h.	Flin et al., 2011
H05-G	MF	9.46	Grain coarsening of water-saturated snow and drainage after 142h.	Flin et al., 2011
Chamair	MF	10	Grain coarsening of water-saturated snow and drainage.	Coléou et al., 2001
E2b	FC	4.91	3 weeks under a TG = 16 K m^{-1}, T_{mean} = -3°C, sampled in the middle of the layer.	Flin et al., 2008
0A	RG	8.392	Sieved snow, following by isothermal conditions.	This study
1A	RG	8.395	3 days under a TG = 43 K m^{-1}, T_{mean} = -4°C, sampled in the middle of the layer.	This study
2A	FC	8.373	6 days under a TG = 43 K m^{-1}, T_{mean} = -4°C, sampled in the middle of the layer.	This study
3A	DH	8.400	9 days under a TG = 43 K m^{-1}, T_{mean} = -4°C, sampled in the middle of the layer.	Calonne et al., 2011
4A	DH	8. 397	13 days under a TG = 43 K m^{-1}, T_{mean} = -4°C, sampled in the middle of the layer.	Calonne et al., 2011
5A-G	DH	9.655	17 days under a TG = 43 K m^{-1}, T_{mean} = -4°C, sampled in the middle of the layer.	This study
7A-G	DH	9.672	21 days under a TG = 43 K m^{-1}, T_{mean} = -4°C, sampled in the middle of the layer.	This study
Grad3	DH	10	8 days under a TG = 100 K m^{-1}, T_{mean} = -5°C.	Coléou et al., 2001

Table 1: List of the 35 snow samples used in the present work. Snow type is defined according to the International Classification for Seasonal Snow on the Ground [*Fierz et al., 2009*]: PP, Precipitation Particles; DF, Decomposing and Fragmented precipitation particles; RG, Rounded Grains; FC, Faceted Crystals; DH, Depth Hoar; MF, Melt Forms. Lines with gray background correspond to samples for which detailed information is provided below.

[1] 1325 m altitude, Chartreuse range, France.
[2] 3200 m altitude, Ecrins range, France.

Computed Values for the 35 Samples Used in the Study

Sample name	Snow type	K_x x 10^{-9} (m^2)	K_y x 10^{-9} (m^2)	K_z x 10^{-9} (m^2)	SSA (m^2 kg^{-1})	Density (kg m^{-3})
Fr	PP	3.58	3.77	3.69	55.30	120.49
I01	PP	3.83	2.22	3.33	55.79	102.90
I03	PP	3.79	3.93	4.03	41.37	123.34
I04	PP	4.23	4.16	4.06	42.48	113.43
I08	DF	4.60	4.38	4.79	29.32	147.71
I15	RG	4.54	4.70	4.79	23.32	172.76
I19	RG	4.73	4.82	4.84	19.90	192.48
I21	RG	4.73	4.93	4.36	19.23	198.62
I23	RG	2.82	2.62	2.47	17.24	256.30
P03	PP	2.42	2.38	2.06	50.91	134.55
P04	DF	6.14	6.38	4.62	25.36	157.54
P06	RG	0.64	0.65	0.59	21.59	354.51
P07	RG	2.45	2.44	1.83	17.15	280.05
P08	RG	1.09	1.08	0.96	14.57	379.00
P09	RG	1.26	1.29	1.04	12.29	396.14
P10	RG	1.55	1.68	1.38	10.46	396.07
P11	RG	0.46	0.45	0.40	20.76	413.75
P14	RG	0.90	0.88	0.80	18.13	352.68
P15	RG	1.54	1.54	1.73	16.09	315.54
H00	RG	0.45	0.44	0.43	17.34	431.36
H01	MF	0.48	0.45	0.48	6.99	550.93
H1-2	MF	0.75	0.75	0.74	7.69	503.80
H02	MF	1.22	1.22	1.27	6.18	471.70
H03	MF	1.80	1.88	1.73	5.25	498.11
H05-G	MF	3.96	4.57	4.87	3.78	471.70
Chamair	MF	0.57	0.51	0.54	8.49	525.90
E2b	FC	5.71	4.87	5.62	15.43	239.70
0A	RG	0.76	0.78	0.70	27.68	314.81
1A	RG	1.75	1.74	1.64	23.37	275.01
2A	FC	1.95	1.95	2.02	20.75	282.71
3A	DH	2.98	2.89	3.08	18.18	274.82
4A	DH	2.71	2.61	3.18	15.19	315.36
5A-G	DH	3.77	3.70	4.39	14.89	284.09
7A-G	DH	3.92	3.95	4.84	13.42	311.23
Grad3	DH	0.65	0.63	1.06	21.84	369.18

Table 2: List of the snow samples and types with the corresponding computed values of the permeability in the x, y and z direction (K_x, K_y and K_z), the Specific Surface Area (SSA) and the density. All these values were computed on the largest volume available of each sample, which is at least equal to the REV of the three variables. Snow type is defined according to the International Classification for Seasonal Snow on the Ground [Fierz et al., 2009]: PP, Precipitation Particles; DF, Decomposing and Fragmented precipitation particles; RG, Rounded Grains; FC, Faceted Crystals; DH, Depth Hoar; MF, Melt Forms. Lines with gray background correspond to samples for which detailed information is provided below.

Sample *Fr* - Precipitation Particles (PP)

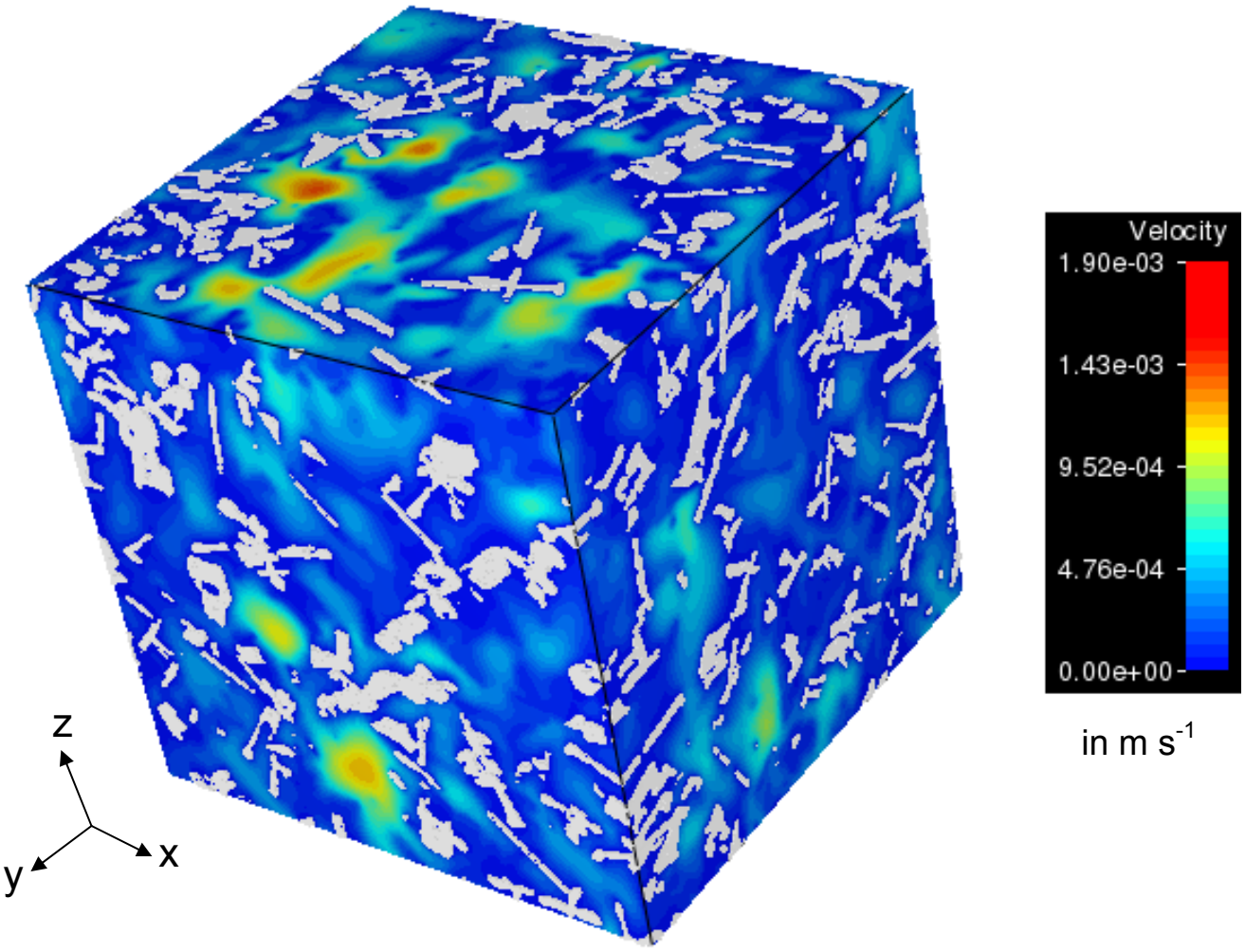

Figure 1.a: 3-D visualization of the fluid velocity for a pressure drop along z direction (size = 750^3 voxels, 1 vox. = 4.91 µm).

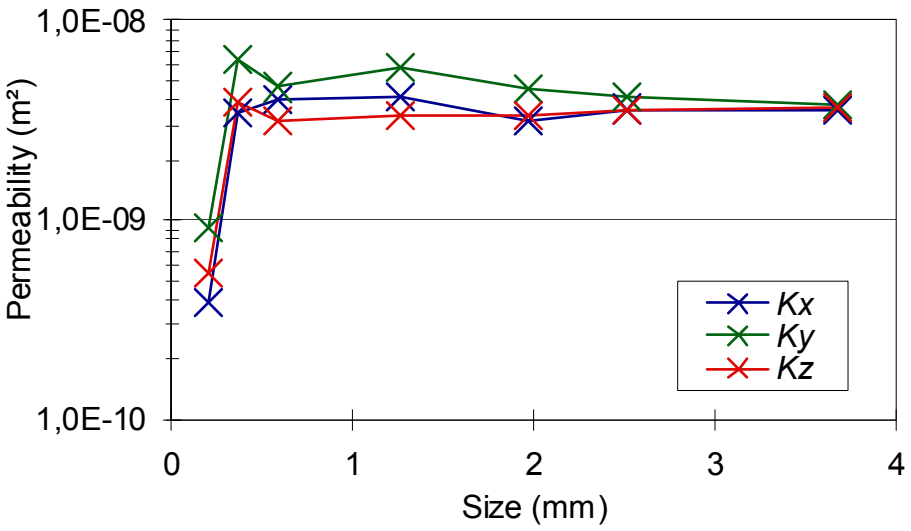

Figure 1.b:
Dependency of **K** estimates with sample size.

Sample *P04* - Decomposing and Fragmented precipitation particles (DF)

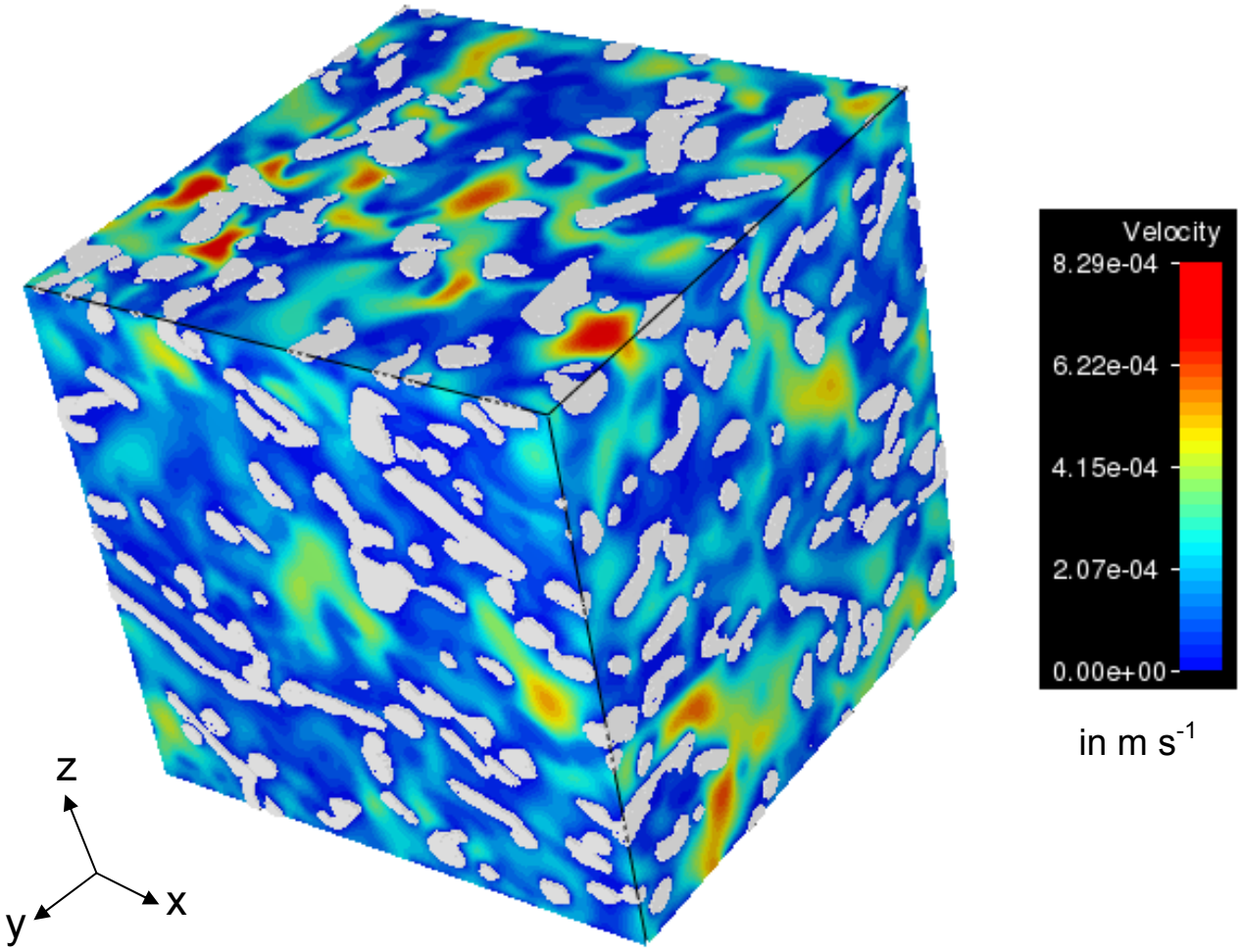

Figure 2.a: 3-D visualization of the fluid velocity for a pressure drop along z direction (size = 512^3 voxels, 1 vox. = 8.588 µm).

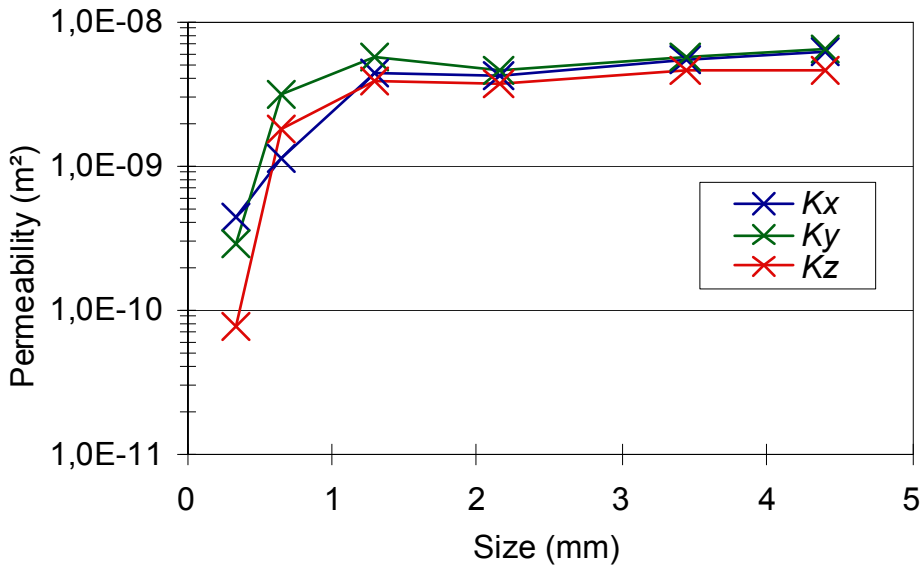

Figure 2.b:
Dependency of **K** estimates with sample size.

Sample *P11* - Rounded Grains (RG)

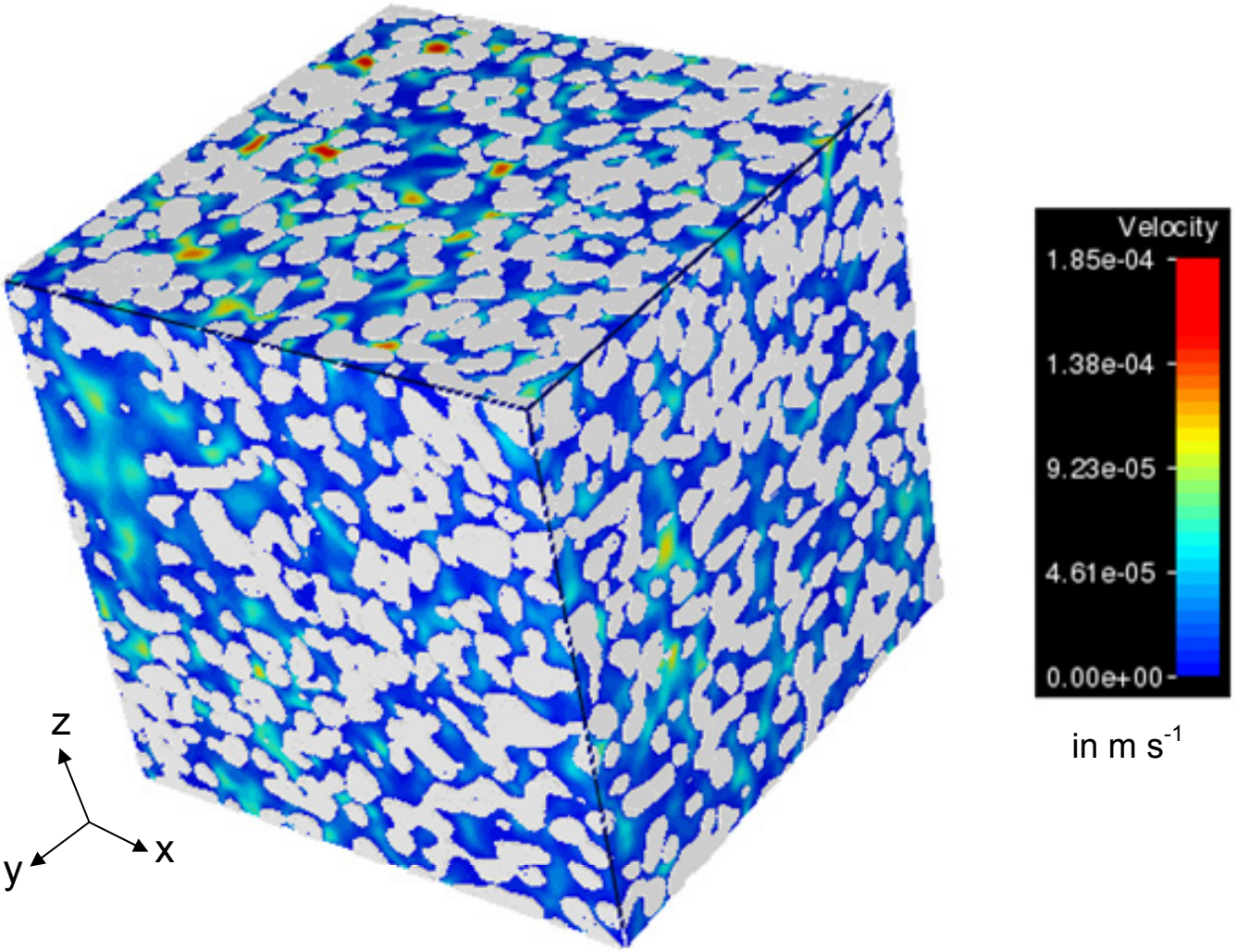

Figure 3.a: 3-D visualization of the fluid velocity for a pressure drop along z direction (size = 512^3 voxels, 1 vox. = 8.588 µm).

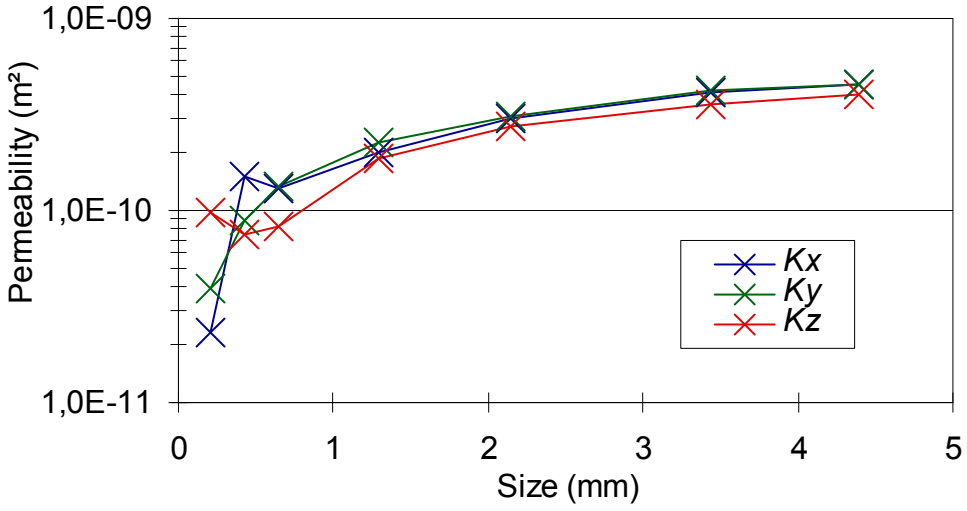

Figure 3.b:
Dependency of **K** estimates with sample size.

Sample *H02* - Melt Forms (MF)

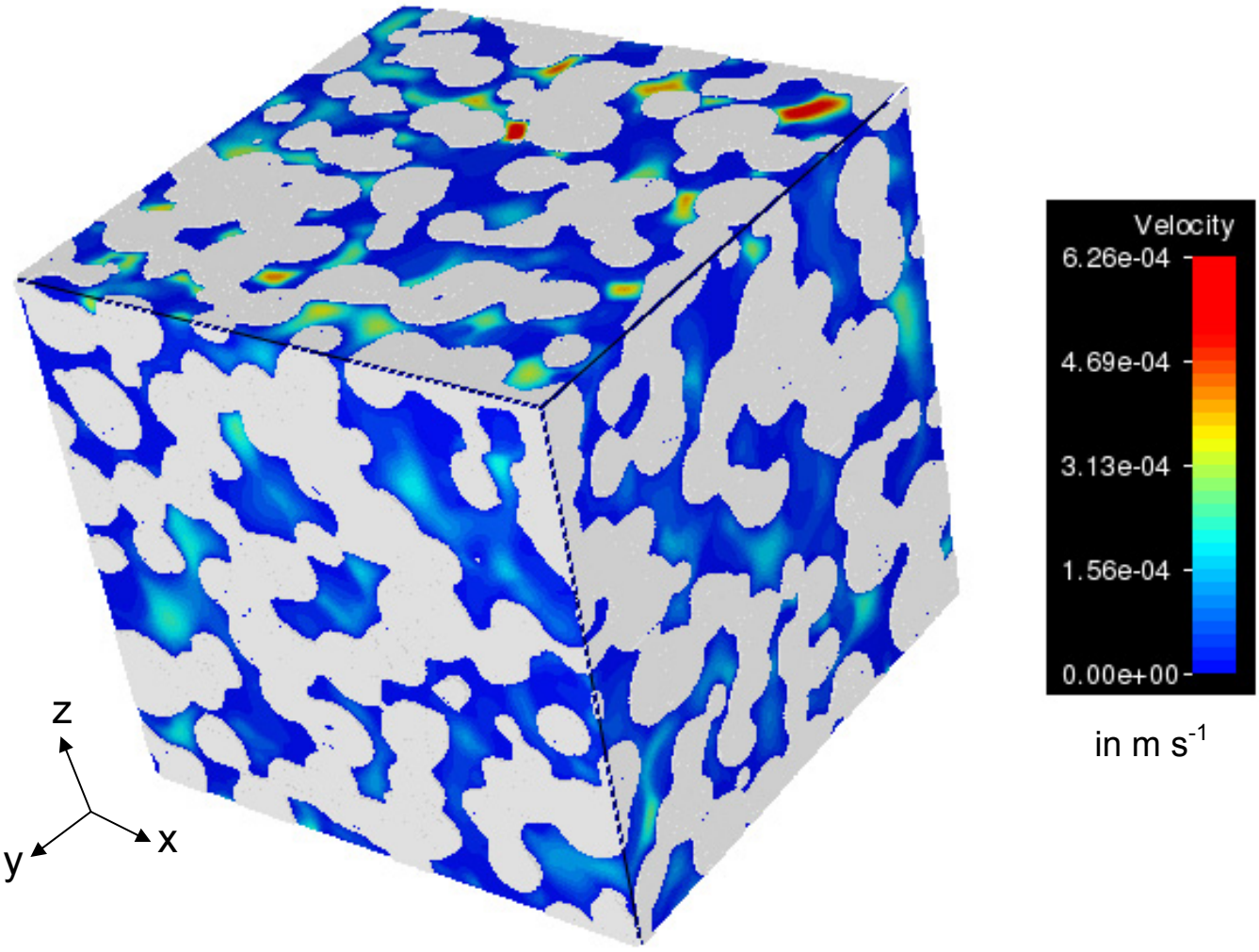

Figure 4.a: 3-D visualization of the fluid velocity for a pressure drop along z direction (size = 651^3 voxels, 1 vox. = 8.590 µm).

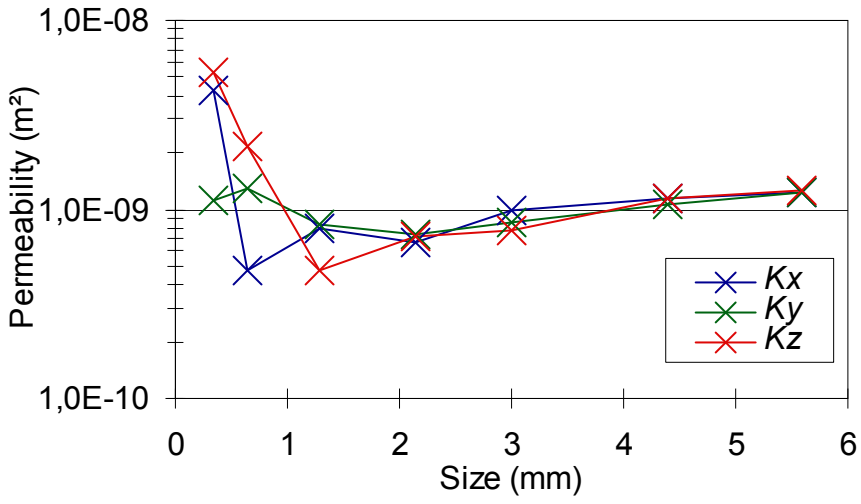

Figure 4.b:
Dependency of **K** estimates with sample size.

Sample *E2b* – Faceted Crystals (FC)

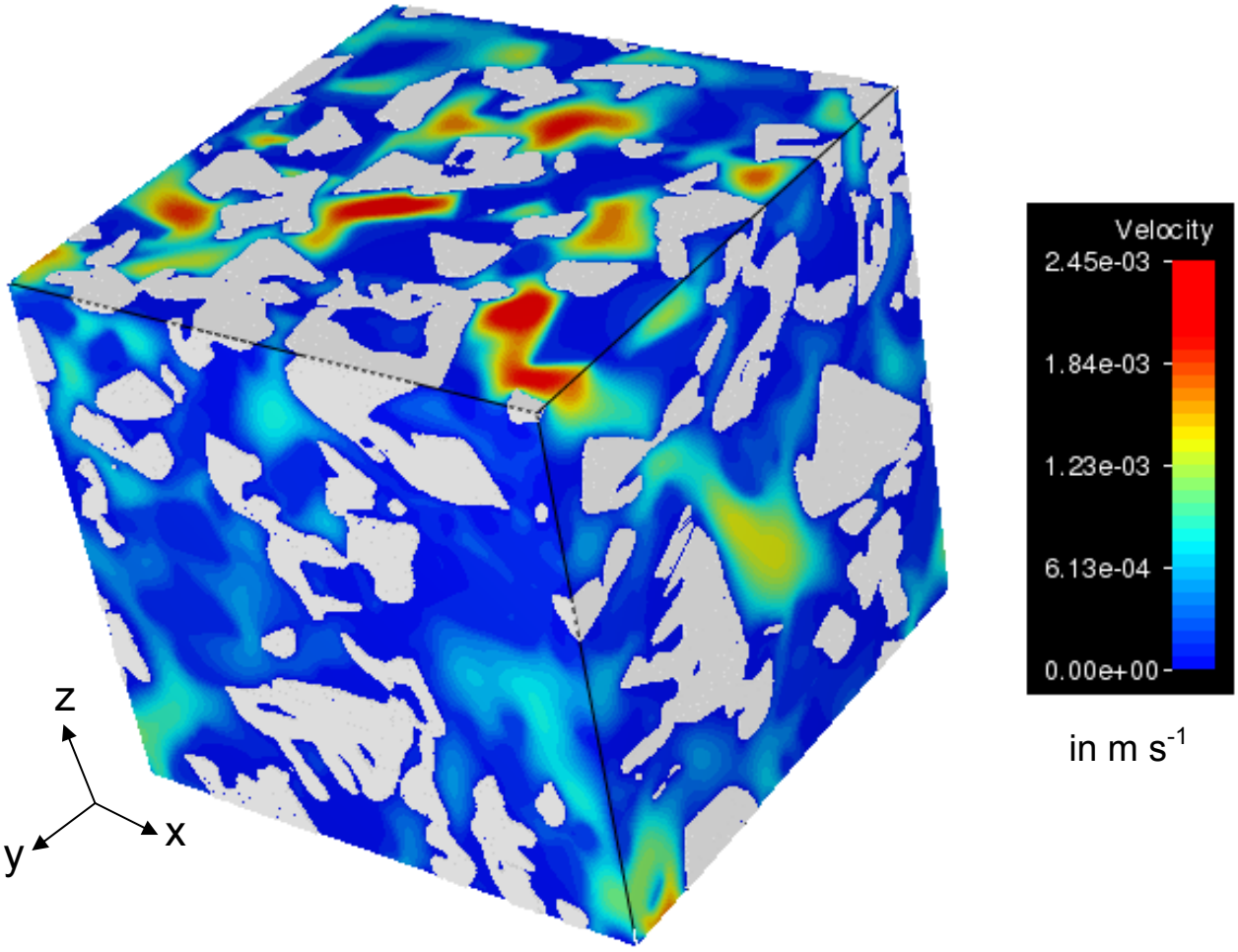

Figure 5.a: 3-D visualization of the fluid velocity for a pressure drop along z direction (size = 750^3 voxels, 1 vox. = 4.91 µm).

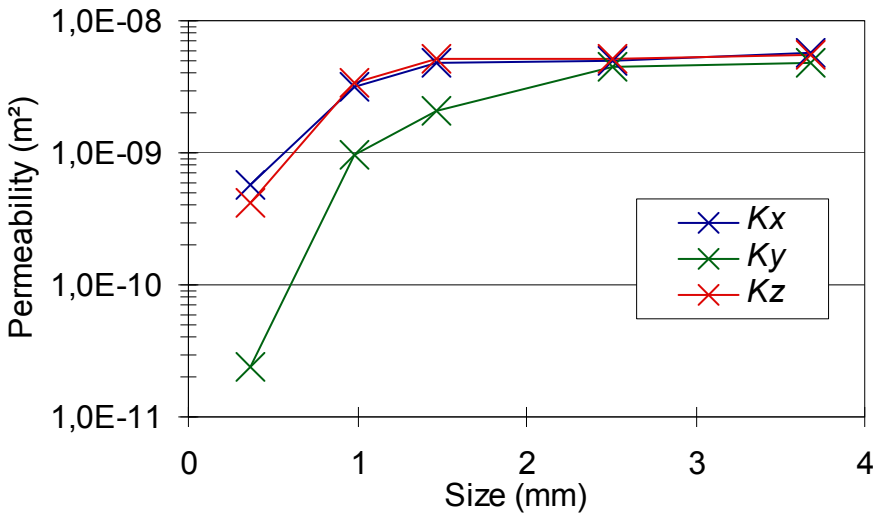

Figure 5.b:
Dependency of **K** estimates with sample size.

Sample *Grad3* – Depth Hoar (DH)

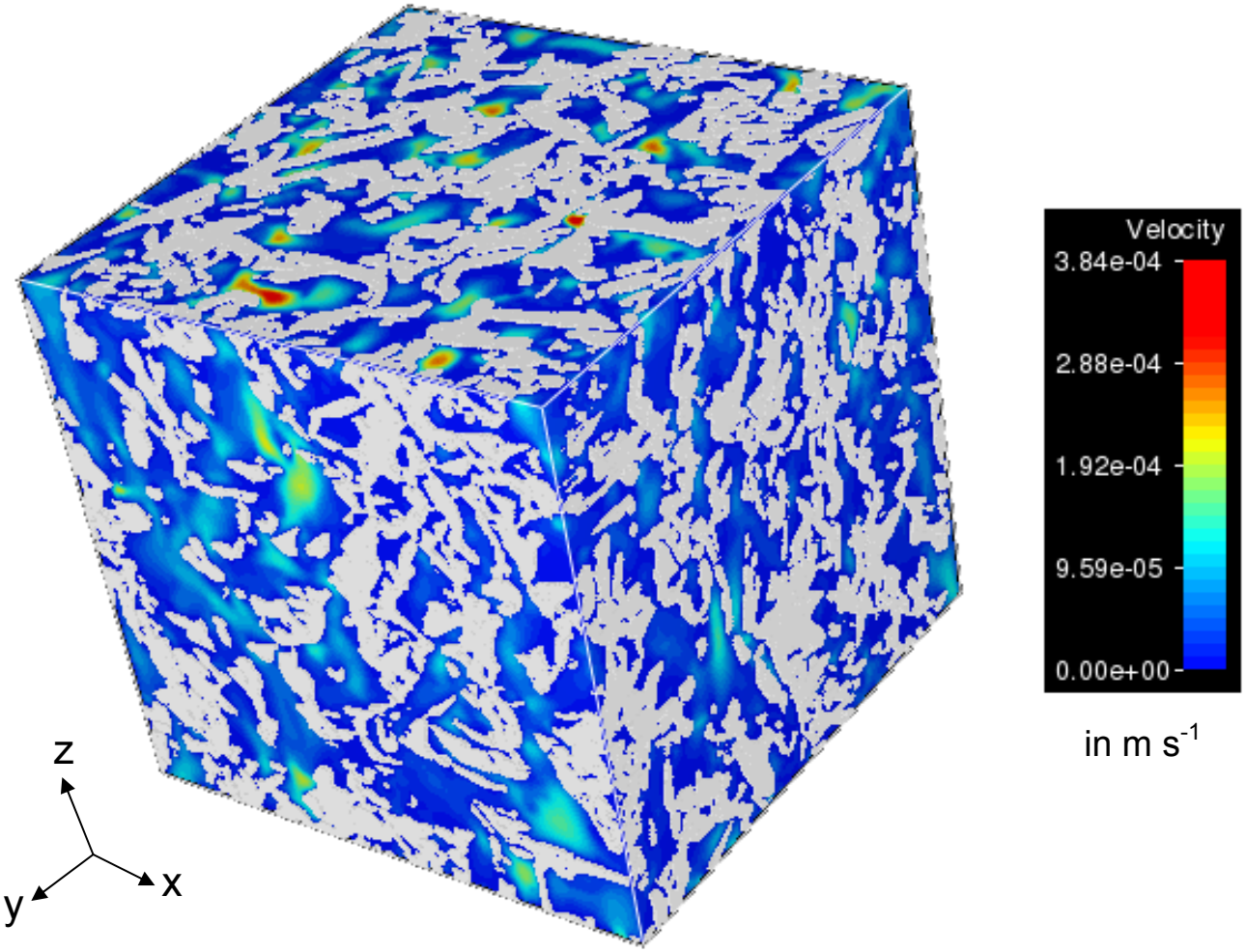

Figure 6.a: 3-D visualization of the fluid velocity for a pressure drop along z direction (size = 600^3 voxels, 1 vox. = 10 µm).

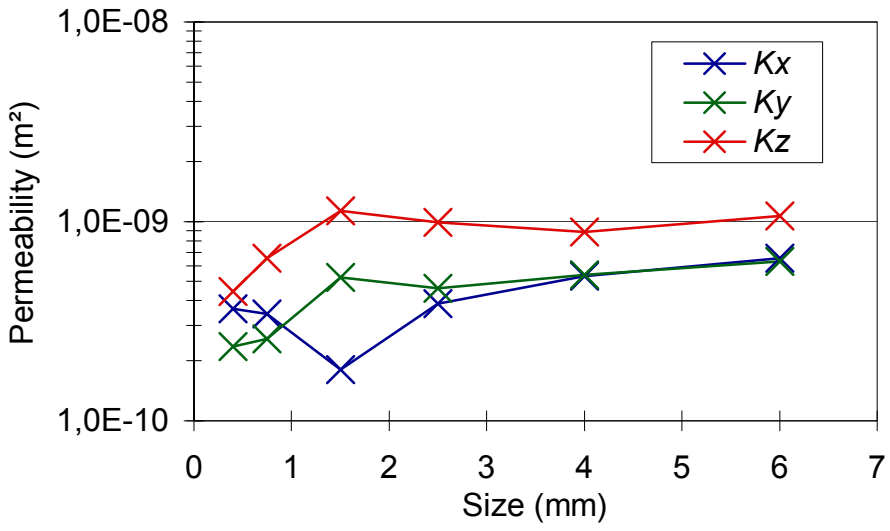

Figure 6.b:
Dependency of **K** estimates with sample size.